Available online at www.sciencedirect.com
SCIENCE DIRECT®
Biomaterials 24 (2003) 2233–2243
Biomaterials
www.elsevier.com/locate/biomaterials

Processing–microstructure–property relations in HVOF sprayed calcium phosphate based bioceramic coatings

K.A. Khor[a,*], H. Li[a], P. Cheang[b]

[a] School of Mechanical & Production Engineering, Nanyang Technological University, 50 Nanyang Avenue, Singapore 639798, Singapore
[b] School of Materials Engineering, Advanced Materials Research Centre (AMRC), Nanyang Technological University, 50 Nanyang Avenue, Singapore 639798, Singapore

Received 29 October 2002; accepted 19 January 2003

Abstract

Hydroxyapatite (HA) based bioceramic coatings were deposited onto titanium alloy substrates using the high velocity oxy-fuel (HVOF) spray technique. This study aimed to reveal the relations among processing parameters, microstructure, and properties of the bioceramic coatings. The processing conditions were altered through changing the starting HA powder size, content of bioinert ceramic additives or composite powder preparation techniques. Coating structure was characterized through scanning electron microscopy (SEM) and transmission electron microscopy (TEM); and the mechanical properties, Young's modulus and fracture toughness, of the coatings were evaluated through indentation techniques. Results demonstrated dominant influence of the melt state of HA powders on the phase composition of resultant coatings, and it was found that the HVOF HA coatings possess competitive mechanical properties. Furthermore, addition of titania or zirconia, as secondary phase in HA, showed promising effect on improving the mechanical properties of the HVOF HA-based coatings. Chemical reactions between HA and titania; and, HA and zirconia during coating deposition were revealed and characterized. Incorporation modes of the additives into HA and their reinforcing mechanisms were elucidated. The relationship among the processing, microstructure, and mechanical properties of the HVOF sprayed bioceramic coatings was summarily examined.

Keywords: Hydroxyapatite; HVOF; Composite coating; Processing; Microstructure; Property

1. Introduction

The predominant purpose of biomaterials is to produce a part or facilitate a function of the human body in a safe, reliable, economical, and physiologically acceptable manner [1]. A prerequisite for any synthetic material implanted in the body is that it should be biocompatible in the sense of not producing an inflammatory tissue reaction. In addition, the implanted material is expected to withstand applied physiological forces without substantial dimensional changes, catastrophic brittle fracture, or fracture in the long term from creep, fatigue, or stress corrosion [2]. Accordingly, hydroxyapatite (HA) coatings, which have been extensively proposed as implants for bone and joint replacements [3–5], must possess acceptable biocompatibility and mechanical performances. Previous in vitro and in vivo tests have revealed that biological performances of HA coatings were significantly related to their phase compositions [5,6]. In order to achieve quick remodeling and fixation with surrounding bone, the implant must meet with limited dissolution post implantation. It has been clarified that the dissolution was dependent on the phases especially those located at the coating surface [6–8]. It is known that dissolvability of the miscellaneous phases possibly existing in a HA coating can be remarkably different. Indeed, the dissolvability hierarchy amongst Ca–P phases has been established to proceed in the order ACP > TTCP > TCP > HA [6]. Even though phase composition of starting HA powders can be ascertained as pure crystalline, nonetheless due to the intrinsic characteristics of the thermal spray process, phase transformation in HA cannot be effectively avoided during the spray. Suitable thermal spray

*Corresponding author. Tel.: +65-6-790-5526; fax: +65-6-791-1859.
E-mail address: mkakhor@ntu.edu.sg (K.A. Khor).

0142-9612/03/$ - see front matter © 2003 Elsevier Science Ltd. All rights reserved.
doi:10.1016/S0142-9612(03)00027-9

processing, optimized spray conditions, and apt powder preparation are hence essentially required. High velocity oxy-fuel (HVOF) spray is expected to be a promising technique for HA coating deposition because it can deposit HA with similar set of advantages that plasma spraying can without the debilitating phase transformations, especially with decreased amorphous calcium phosphate (ACP) content [9,10], following thermal decomposition of HA.

Mechanical properties of HA coatings are crucial to the long term survivability of the implants. Hence, the enhancement of mechanical properties of HA coatings through appropriate addition of bioinert ceramics could help extend the application of HA coatings to, medium to high load regions of the human skeletal system. Besides the contribution of altered spray technique to improve the mechanical properties of HA coatings, incorporation of alternative osteogenic materials such as bioinert ceramics did also showed promising effect [11–13]. Positive effect of yttria stabilized zirconia (YSZ) addition on bending strength of sintered HA [14] and plasma sprayed HA [15] was revealed and, titania incorporation also demonstrated remarkable influence on HA microstructure during sintering [16,17]. However, the reinforcing mechanism of the bioinert ceramics in the HA-based coating is still not firmly established. Moreover, it is obvious that different processing conditions of the coatings should correspond to remarkably different microstructure, and, hence different properties. A systematic study on the effect of processing and microstructure on properties of the HA-based bioceramic coatings is beneficial for a good understanding of the bioceramic coating system and hence, its possible future use in biomedical applications.

In the present study, HVOF sprayed HA coatings were investigated in terms of structure characterization and mechanical property evaluation. YSZ and titania powders were incorporated into HA coatings, respectively, to produce HA-based composite coatings. The incorporation modes were discussed in the present study. The relationship among all the investigated variables, especially microstructure–mechanical property relationship, was discussed.

2. Experimental setup

Starting HA powders were made through a wet chemical method subsequently followed by a spray drying process, using a rotary atomising head, to achieve near-spherical shape with a narrow size profile [18]. Additional annealing heat-treatment at 900°C for 1.5 h was conducted to obtain a crystalline HA structure. In order to reveal the influence of processing conditions on coating properties, three types of HA powders in terms of different particle size ranges were sprayed. These were $50 \pm 10\,\mu m$ (Type A), $40 \pm 10\,\mu m$ (Type B) and, $30 \pm 10\,\mu m$ (Type C). The titania powders employed in the present study were composed of pure anatase phase. The commercial powder size were approximately 1 μm. Yttria stabilized zirconia (YSZ, 8 wt% yttria) powders (Praxair Thermal Inc., IN, USA) with an average particle size of 35 μm were ball milled in a zirconia planetary jar at a milling speed of 100 rpm for 3 h. The final particle size of the YSZ powders had an average size of 3 μm. The size distribution of all the powders employed in the present study was determined using a laser particle size analyzer, Analysette 22, Fritsch Gmbh, Germany. The composite coatings with the composition 90 vol% HA + 10 vol% titania, 80 vol% HA + 20 vol% titania, and 90 vol% HA + 10 vol% YSZ, were deposited using mechanically blended powders. A fully computerized HV2000 HVOF system (Praxair, USA) with a nozzle diameter of 19 mm was used in the present study. The spray parameters of HVOF together with those of plasma spray, which was used for the spheroidization described below, are tabulated in Table 1. The present spray parameters were selected according to previous preliminary experiments. In order to reveal the influence of incorporation modes on strengthening effect of the additives on HA-based coatings, the composite powders made from slurry-spheroidization were also prepared and typically sprayed to form composite coatings. During the slurry-spheroidization process, the YSZ powder and titania powder were mixed correspondingly with HA feedstock (with an average particle size of 40 μm) in distilled water with PVA binder to form a viscous solution. Subsequently, the slurry was stirred for 5 h to obtain uniform mixing. Removal of the organic binder was achieved through heat treatment at 450°C in an electrical resistant furnace for 1 h, and thereafter, heated to 600°C for 6 h for the purpose of intra-particle consolidation. Separate slurry particles were obtained using mortar and pestle; and ensuing ball milling at 100 rpm for 2 h. A 40 kW DC plasma spray system (SG-100, Praxair Thermal, USA) was employed in the present study to accomplish the spheroidization process for the HA/titania and HA/YSZ composite powders via the slurry route. The plasma spray parameters are listed in Table 1. Titanium alloy, Ti–6Al–4V, was used as substrates. Flat plate samples, with dimensions of $100 \times 20 \times 2\,mm^3$ in length, width and thickness, respectively, were employed for coating deposition.

Surface and cross-sectional morphology of the coatings was observed by means of scanning electron microscope (SEM, JEOL JSM-5600LV) and; transmission electron microscope (TEM, JEOL, JEM-2010) at 200 kV. The cross-sectional morphology of the coatings was observed using the TEM. With regards to the inherent brittleness of HA, the TEM samples were prepared on special copper slots ($2 \times 1\,mm^2$ in size) and

Table 1
Spray parameters of HVOF and plasma spray

HVOF	Plasma spray (for the spheroidization)
Flow of H_2: 56 l/min	Net energy: 2 kW
Flow of O_2: 283 l/min	Flow of Ar: 28.30 l/min
Spray distance: 250 mm	Flow of He: 18.87 l/min
Flow of Ar (powder carrier gas): 19 l/min	Distance from water: 200 mm
Powder feeding rate: 8 g/min	Flow of Ar (powder carrier gas): 9.43 l/min
	Powder feeding rate: 8 g/min

followed by polishing and ion milling processes. Phase composition of the starting powders and as-sprayed coatings was analyzed by X-ray diffraction (XRD) (MPD 1880, Philips, the Netherlands). The operating conditions were 40 kV and 30 mA by using Cu Kα radiation. The goniometer was set at a scan rate of 0.015°/s over a 2θ range of 20–60°. Quantitative phase analysis on investigated crystalline coatings was conducted using Rietveld method [19,20]. High temperature differential scanning calorimetry (DSC, Netzsch Thermal Analysis, DSC 404C, Germany) was utilized for the characterization of thermal behavior of the powders at elevated temperatures. The DSC test used nitrogen gas with a flow rate of 150 ml/min as the analysis atmosphere. Fractures toughness and Young's modulus of the investigated coatings were also determined in the present study. Indentation technique was employed for the fracture toughness determination and 3-point bend test was used to measure the Young's modulus (E) of the bulk coatings. Both techniques have been elaborated in a previous paper [21]. The indentation test was conducted on fine polished cross-sections (using 1 μm diamond paste) of the coatings, and a Vickers load of 0.5 N was thereafter applied on the samples with a load application duration of 15 s. A total of 15 points were collected for each type of coating. The experiment was conducted on the HMV-2000 Shimadzu microhardness tester. The 3-point bend test was carried out on double-side sprayed specimen so that the symmetry can be ascertained while the coatings on both sides are of the same thickness. The dimension of the substrate for 3-point bending test was $120 \times 20 \times 2\,mm^3$ in length, width and thickness, respectively. The coatings had a thickness of 180 ± 10 μm. Three samples were prepared for the bending test for each type of coatings. Three bending curves were obtained by choosing different positions for every sample. The tests were performed using Instron universal testing machine and the bending rate employed was 0.2 mm/min. Subsequently, a set of load–displacement data was chosen for the calculation of E within the elastic deformation regime.

3. Results and discussion

3.1. X-ray diffraction

XRD plots of as-sprayed HA coatings investigated are shown in Fig. 1. It reveals that, besides the peaks designated to crystalline HA, the peaks belonging to α-TCP ($Ca_3(PO_4)_2$) are found in all the as-sprayed coatings. It is noted that, apart from the different amount of TCP, different crystallinity values can be induced from the XRD patterns. Smaller initial HA powders brought about lower crystallinity in the as-sprayed coatings. Using XRD area integration method [22], the crystallinity of the three types of coatings was determined using the main peak [2 1 1]. It reveals that, under the same spray conditions, Types A, B, and C coatings have the crystallinity values of 95%, 85%, and 41%, respectively. It has been widely reported that α-TCP was formed in the as-sprayed coatings due to HA phase decomposition [23,24]. The increased content of such phase in the coatings made from small HA powders (Type C) indicate extensive transformation of HA during the spraying. Moreover, it is also noted that in the coating made from 40 μm HA powders (Type B), a trace of TTCP appeared, while in Type C coating, made from the smallest HA powders, a small amount of β-TCP was detected. The presence of TTCP and β-TCP suggests that further heating of HA could result in further phase transformation to TTCP. This point has been reported in Ref. [25] that transformation of HA to TTCP occurred at about 1360°C through some transient phases. The appearance of β-TCP is possibly attributed to the phase transformation from α-TCP at about 1100°C [26]. It should be noted that TTCP and β-TCP were only detected in the coatings made from small HA powders (Types B and C). This may suggest the influence

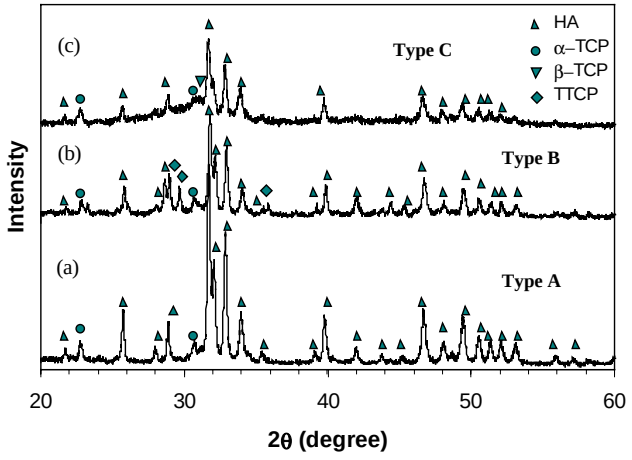

Fig. 1. XRD plots of the HVOF sprayed pure HA coatings showing the influence of particle size of the starting powders on phase composition of resultant coatings, the powder size is: (a) 50 ± 10 μm, (b) 40 ± 10 μm, and (c) 30 ± 10 μm.

of the melt state of HA powders on subsequent cooling rate upon impingement, which could determine further phase transformation besides α-TCP. This point was proved by other studies that once HA powders were totally melted, in the resultant coating, the phases, α-TCP, TTCP and β-TCP, are all exhibited [27]. The difference in the content of α-TCP in the coatings demonstrated in Fig. 1 further indicates that the extent of HA phase decomposition may possibly be substantially related to the melt state of the powders during coating formation.

3.2. Electron microscopy of HA powders and coatings

Analysis on HVOF sprayed HA powders suggests remarkable different melt states of the particles. The spheroidised particles were collected through spraying the powders into distilled water, thereafter collected and, dried for further analysis. The melt state of the powders can be verified through observing the polished cross-sectional morphologies in a SEM, which are shown in Fig. 2. It is observed that the large powders are only partially melted, which can be affirmed by the resolidified shell of the powders (Fig. 2a). For the small HA powders, near-fully melted state is demonstrated (Fig. 2c). Since the detachment of the unmelted layers within the particle may occur during the sample preparation, the melted shell of a single particle remained in the specimen (Fig. 2b). A statistical observation of a large quantity of particles states that increase of powder size results in decrease of melting fraction. It is nevertheless believed that powders' melt state should be responsible for the final coating microstructure. From this point of view, the melt fraction of powder is practically meaningful. Therefore, to achieve high crystallinity of the coating, which is required for a quick fixation of the coating during their service as implants in biomedical applications, appropriate powder size together with apt HVOF spray parameters must be carefully selected. The coating morphology shown in Fig. 3 further reveals the influence of the melt state on grain size of the coatings. It clearly demonstrates the interface zone between melted and unmelted parts within a HA splat. It is noted that the HA grains located in unmelted part are of far larger size than those in melted part (Fig. 3), which states the influence of rapid cooling on grain growth during coating formation. The relatively reduced grain size located in the resolidified zone, which is around splats' interface, should act as an important factor contributing to the improved mechanical properties. TEM observation also clarifies that most of TCP phase observed reside in region where HA decomposed. It is therefore believed that the melted portion of the powder is in direct response to the formation of amorphous phase. The crystalline HA can be attributed to the original HA phase in the starting powders. The α-TCP, β-TCP, or TTCP phases could also have resulted from the decomposition of the powders at the melted region.

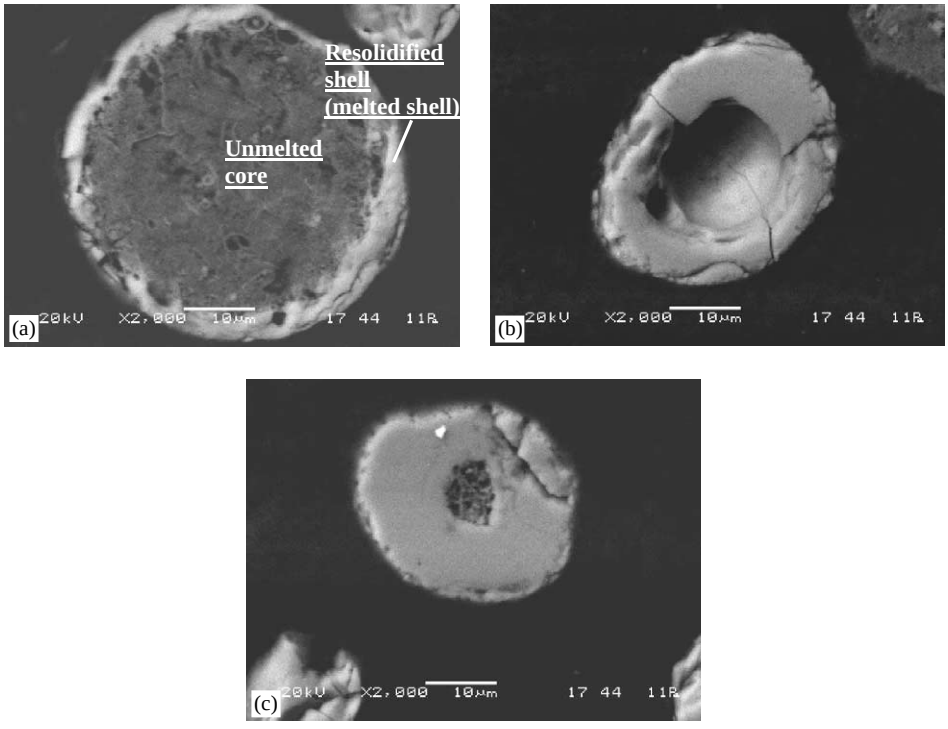

Fig. 2. Cross-sectional morphology of HVOF sprayed HA particles showing their different melting fraction depending on their size under the same spray conditions.

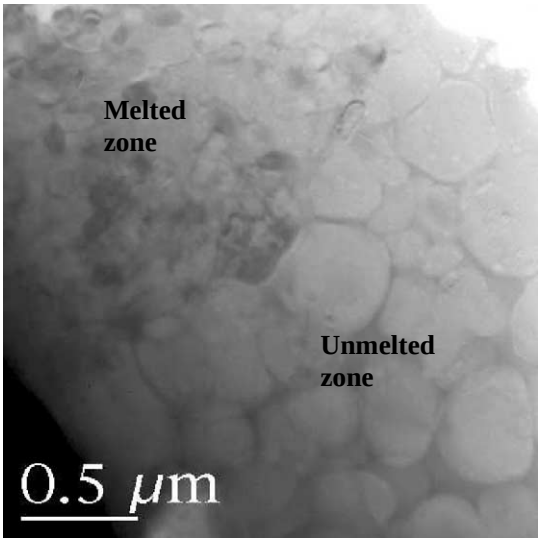

Fig. 3. TEM image of as-sprayed HA coating showing the interface between melted and unmelted parts within a HA splat and different grain size.

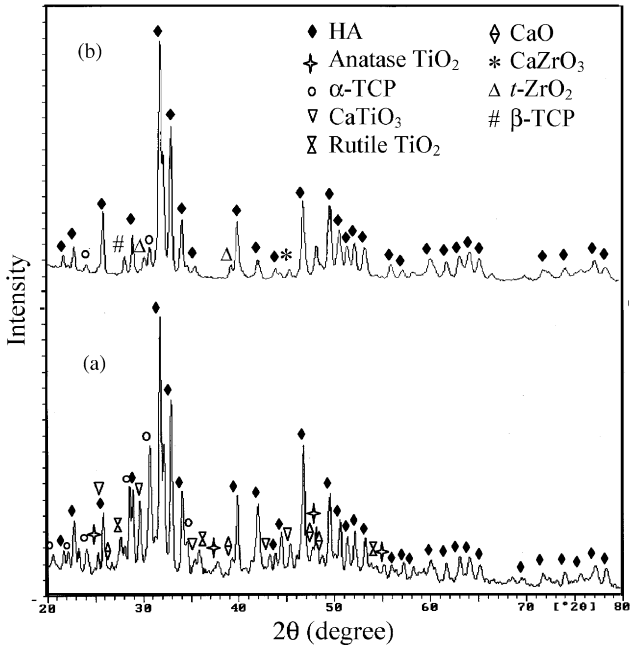

Fig. 4. XRD patterns of HVOF sprayed HA/10 vol% titania coating (a) and HA/10 vol% YSZ coating (b) using the mechanically blended powders.

Fig. 4 shows the XRD patterns of the HA/titania and HA/zirconia composite coatings. It is evident that chemical reactions between the components, namely HA with titania, and HA with zirconia, took place during coating deposition, which are indicated by the appearance of $CaTiO_3$ and $CaZrO_3$ respectively. The following formula is suggested for illustrating the chemical reaction between HA and titania

$$Ca_{10}(PO_4)_6(OH)_2 + TiO_2 \rightarrow 3Ca_3(PO_4)_2(TCP) + CaTiO_3 + H_2O\uparrow \quad (1)$$

Many researchers have analyzed the reaction between HA and *t*-zirconia, which is described as follows [28–30]:

$$Ca_{10}(PO_4)_6(OH)_2(HA) \rightarrow 3Ca_3(PO_4)_2(TCP) + CaO + H_2O\uparrow \quad (2a)$$

$$CaO + ZrO_2 \rightarrow CaZrO_3 \quad (2b)$$

During the composite coating formation, phase decomposition of HA also took place in the form of Eq. (2a). However, compared to pure HA coating which is also made from the same HA powder size, TTCP is not present in the composite coatings. This phenomenon may suggest coexistence of either titania or zirconia with HA has beneficial effect in inhibiting its further phase transformation.

3.3. Differential scanning calorimetry (DCS)

In order to fully understand the influence of the additives on thermal behaviors of HA at high temperatures, high temperature DSC test was conducted on the composite powders as well as pure HA for comparison. Fig. 5 illustrates the DSC heating curves of all the powders. It was revealed that the starting HA powders (a) and HA/titania powders (b) and HA/zirconia powders (c) show miscellaneous chemical changes except for the peak labeled at around 1457°C, which would be the point where further transformation of HA occurs [31,32]. It is found that HA powders exhibit endothermic characteristic during heating, which spans approximately from 1180°C to 1340°C. These broad peaks may refer to the phase transformation from HA to α-TCP or even $Ca_4O(PO_4)_2$ [23,31]. Beyond 1200°C HA would lose its OH^- groups gradually [31]. The comparison among the mixed powders (b,c) and pure HA powders (a) indicates that the chemical reaction occurs at around 1410°C for HA/titania and 1350°C for HA/zirconia under existing DSC conditions (i.e. N_2 atmosphere). It is obvious that under the present DSC conditions, the reaction between HA and zirconia is very limited, which may be attributed to the limited content of CaO, that in turn can only come about from thermal decomposition of HA. Other reports have pointed out that $CaZrO_3$ has appeared at 1100°C [28] or 1200°C [12] for the HA/YSZ composites, which may depend on how fast phase transformation in HA occurs. It is nevertheless suggested that limited HA phase transformation is a useful way to avoid the chemical reaction between HA and zirconia. It shows that the chemical reaction takes place while the components are in solid state. Based on the present comparative DSC results, it is reasonable to claim that the chemical reaction between

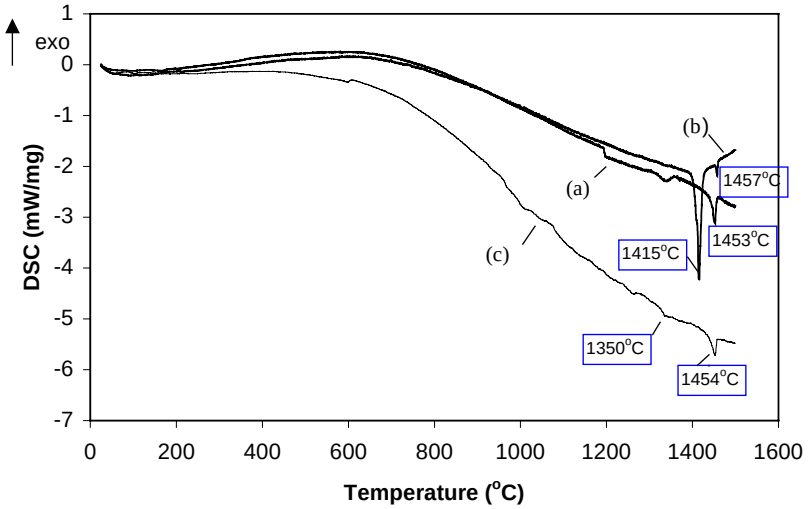

Fig. 5. DSC heating curves of: (a) HA powders, (b) mechanically blended HA/10 vol% titania powders, and (c) mechanically blended HA/10 vol% YSZ powders (heating rate is 10°C/min).

HA and titania takes place at around 1410°C during the HVOF composite coating deposition. The present results also suggest that the existence of either TiO_2 or zirconia powders can effectively inhibit HA phase transformation at temperatures lower than their chemical reaction points, which is indicated by the disappearance of correspondent peaks marked from 1180°C to around 1340°C. Even though Weng et al. [16] reported that HA/titania composites sintered at 900°C with 60 min demonstrated $CaTiO_3$, as a byproduct of the chemical reaction, the long heating duration seems to play an important role in determining the reaction rate, and the temperature at which the reaction occur. Moreover, the particle size of titania and its content in the composites should also be considered.

In order to fully understand the reaction behavior between the components, reaction activation energy between HA and titania was studied. Basically, the activation energy of the chemical reaction between HA and titania can be determined from the DSC curves with various heating rates according to multiple-heating-rate methods [33]. The Kissinger equation was used for the activation energy determination [33]

$$\frac{\mathrm{d}[\ln(\phi/T_\mathrm{r}^2)]}{\mathrm{d}(1/T_\mathrm{r})} = -\frac{Q}{R}, \tag{3}$$

where Q is the activation energy, R is the gas constant (8.31 J/mol K), T_r is the reaction temperature obtained from the DSC test (K), ϕ is the heating rate (K/min). In the present study, the HA/titania composite powders were studied by high temperature DSC with different heating rates. The heating rates, 5, 10 and 15 K/min, were investigated.

The DSC curves under various sample heating rates on the mechanically blended HA and titania powders are shown in Fig. 6. It is found that the reaction temperature changed slightly depending on sample

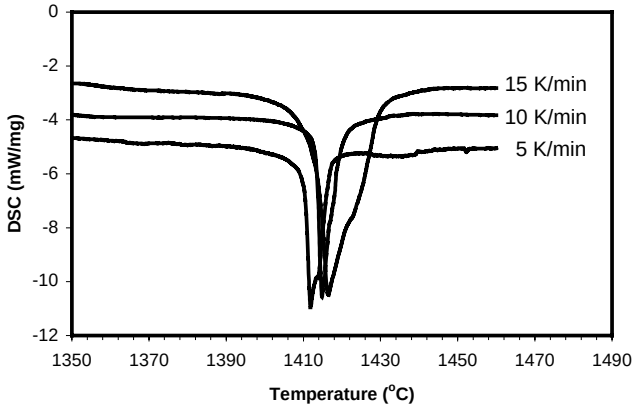

Fig. 6. Effect of heating rate on the mutual reaction temperature between HA and titania.

heating rate: 1411.75°C (5 K/min), 1414.75°C (10 K/min) and 1416.5°C (15 K/min). It is noted that the heating rate shows some effect on the temperature value at which the chemical reaction between HA and titania occurs. According to this multiple-heating-rate method, the activation energy, Q, can be calculated. Fig. 7 shows the regressive curve relating $\ln(\phi/T_\mathrm{r}^2)$ and $1/T_\mathrm{r}$ which were calculated from the DSC results shown in Fig. 6. It is obvious that Q can be determined from the slope of the curve according to Eq. (3). It reveals that the activation energy of the chemical reaction between HA and titania is 5441.46 kJ/mol.

Through spraying either the composite powders into distilled water for analysis, results showed no evidence of chemical reaction between HA and zirconia, or, HA and titania. Therefore, the reaction nevertheless took place during coating formation. It indicates that the chemical reaction has very limited reaction time, which is in response to a limited extent of the reaction. It should be noted that due to the relatively low temperature of HVOF flame (<3000°C), and high

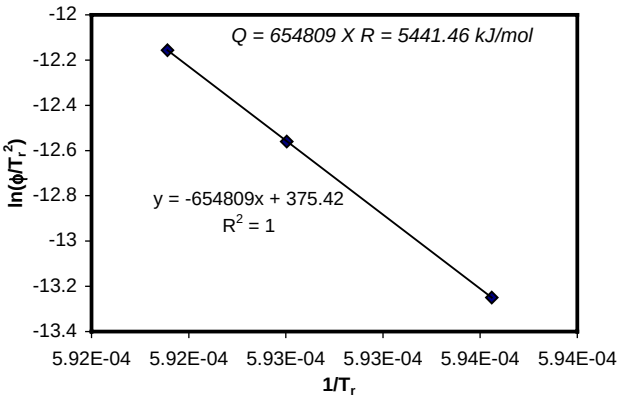

Fig. 7. Activation energy (Q) determination through $\ln(\phi/T_r^2)$ versus $1/T_r$ curve.

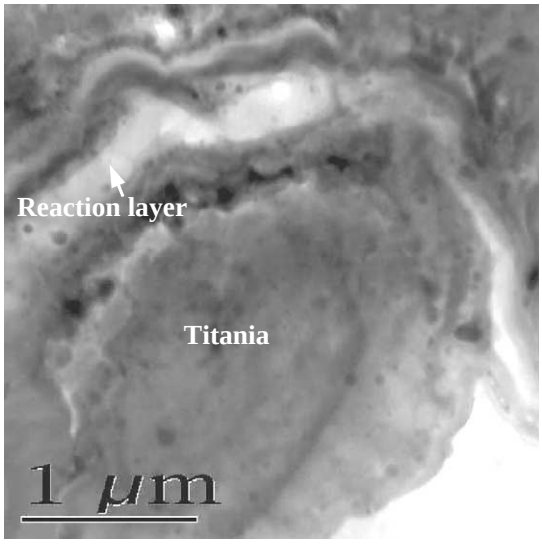

Fig. 8. Morphology of HA/titania composite structure showing that titania is surrounded by a chemical reaction layer with the thickness of around 140 nm.

melting or transformation points of titania and zirconia, the titania and zirconia additives could not be melted during the spraying. The morphology analysis through SEM observation in the present study confirmed that phenomenon. Compared to the extensively used plasma spray process, the present HVOF technique effectively limit both phase transformation of zirconia, which is detrimental for coating structure due to different CTE possessed by different structures, and chemical reaction with HA. The reaction could influence the structure of the accumulated coating. The microstructure of the HA/titania composite coatings is analyzed using TEM, which is shown in Fig. 8. A thin layer ($\sim$120 nm) between HA and titania was revealed. Further EDX detection claims that that layer is the reaction layer, which contains mainly the reaction resultants. It is found that the layer is dense, and it connects the two components together firmly. It therefore can be concluded that limited reaction between the components, HA/titania or HA/zirconia, may have beneficial influence in improving coating structure. Chou et al. [29] studied the microstructure of plasma sprayed HA/zirconia composite coatings in detail and pointed out that $CaZrO_3$ was formed through diffusion of calcium ions to zirconia and, a crystal-orientation relationship between zirconia and $CaZrO_3$ was revealed. However, in the present study, as mentioned above, the chemical reaction can only be possible during the impingement stage, as the splattering of sprayed particles on precoating or substrate is an isolated procedure, the reaction could be very limited and a reaction layer is quite likely the result.

In order to compare the results made from various powder preparation techniques, the composite powders made from slurry-spheroidization was also studied. The present HA/titania composite powders were processed using plasma power 2 kW. The typical surface and cross-sectional morphology of spheroidized HA/TiO_2 and HA/YSZ powders is shown in Fig. 9. A smooth particle surface is clearly observed (the morphology shown in (a)) and, therefore, a densified surface layer around the composite particle induced by plasma spray could be deduced. Figs. 9b and c further reveals the improvement of the components' interface, that is, titania or YSZ powders firmly bond with HA particle. Concerning the partially melt state of HA particle under the present plasma spray conditions, it is possible that the chemical reaction between HA and titania could occur during the spheroidization.

XRD analysis on these spheroidized composite powders, which is depicted in Fig. 10 for HA/titania powders, confirms that prediction. It was revealed that, compared to the raw slurry composite powders after sieving, spheroidized HA/TiO_2 and HA/YSZ powders demonstrate significant chemical reaction, which is suggested by the appearance of large amount of reaction product, $CaTiO_3$ or $CaZrO_3$. In the plasma spheroidized composite powders, the phase composition of crystalline HA, α-TCP and CaO were also detected. It indicates that during the spheroidization process, the chemical reaction between the components took place. Large amount of $CaTiO_3$ or $CaZrO_3$ is not beneficial since these phases have a low degree of bioactivity. Moreover, the present study did not find any effective method to reverse the reaction. Therefore, the powders are essentially deemed as undesirable for coating deposition. Nevertheless, spheroidized HA/10 vol%YSZ powders were HVOF sprayed to reveal further structural changes and changes in mechanical properties. Phase analysis on the coatings showed that content of $CaZrO_3$ increased from 1.15 wt% in the spheroidized powders to 3.37 wt% in the coatings. It alludes to further reaction between zirconia and CaO occurred as extra CaO was released from decomposition of HA during thermal spraying.

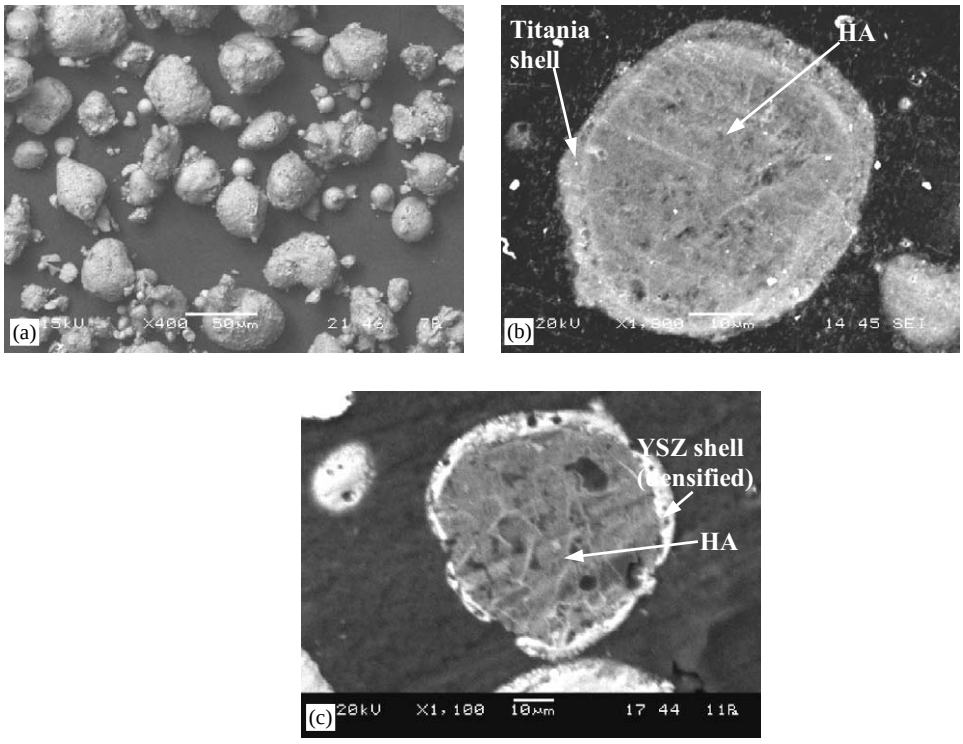

Fig. 9. Typical surface and cross-sectional morphology of spheroidized HA/TiO_2 (a,b) and HA/YSZ composite powders (c) by plasma spraying at the power level of 2 kW.

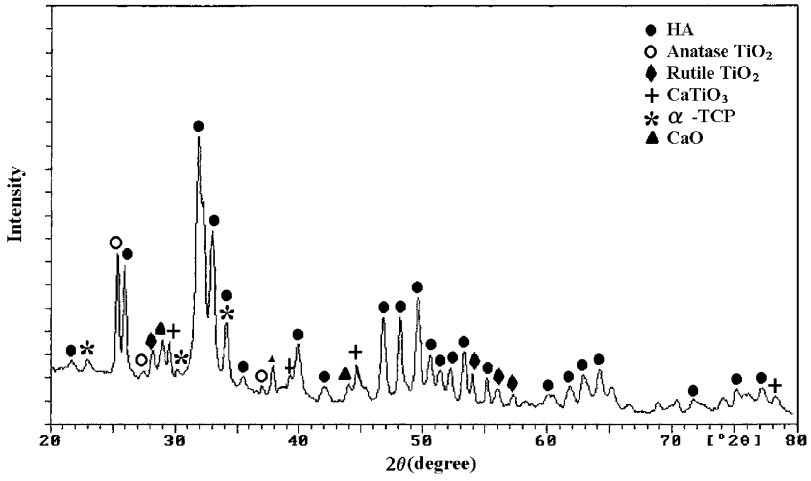

Fig. 10. XRD patterns of typical plasma spheroidized HA/titania powders.

3.4. Mechanical properties

Elastic modulus and fracture toughness of all the coatings investigated are shown in Fig. 11. It shows that addition of titania or YSZ has a positive effect on improving both the Young's modulus and fracture toughness of the coatings. The difference in fracture toughness indicates that the coating microstructure bring about remarkable effect on the fracture behavior. Microstructure observation shows that the cracks induced by the indenter propagate along the splats' interface within the coatings. As shown in Fig. 11, it reveals that small HA powders result in higher fracture toughness. It is believed that fully melted powders could result in a relatively high splats' bonding ratio. As a result, increased interface density can be expected, which was believed to be a predominant beneficial factor influencing fracture toughness [34]. The phases that resulted from thermal decomposition are likely to be located near or even along the splats' interface and, hence effectively contribute to the splats bonding area. Thus, the ability to inhibit crack propagation induced by the indenter could be improved. From this viewpoint, a complete melt state achieved by small HA particles is

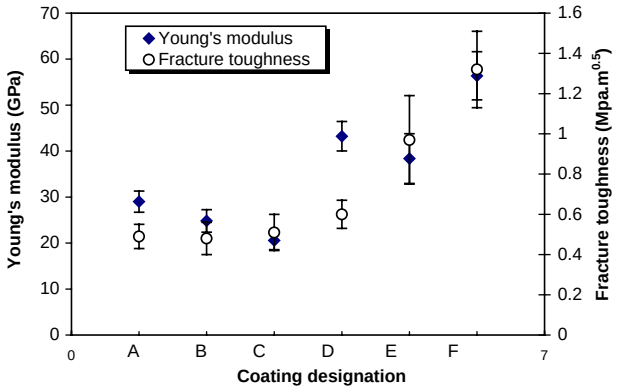

A: HA coating (50 μm), B: HA coating (40 μm), C: HA coating (30 μm), D: HA/10vol.%titania coating (mechanical blended powders), E: HA/10vol.%YSZ coating (mechanical blended powders), F: HA/10vol.%YSZ coating (spheroidized)

Fig. 11. Young's moduli and fracture toughness of the investigated bioceramic coatings.

beneficial for the splats' bonding, and thus, is responsible for the improvement of fracture behavior. The increased Young's modulus and fracture toughness exhibited by the composite coatings indicate the influence of existence of the ceramic as additives and the effects brought about mainly by chemical reaction byproducts. Previous study has also pointed out that the bonding state among splats played an important role as coating microstructure correspondingly influences its E to a large extent [35]. The changes in Young's modulus exhibited by the composite coatings imply the main solitary effect of the ceramic as additives; Young's moduli of titania and zirconia are far higher than that of HA. Furthermore, changes of other variables, such as residual stresses [36] induced by addition of the bioinert ceramics, may also be involved in altering the overall Young's modulus of the coatings. Concerning the principles of the indentation method used for the fracture toughness determination [21], it is obvious that bonding state among the splats is mainly responsible for the ability of the coating to inhibit crack propagation. The chemical reaction between HA and titania, and HA and zirconia contributes significantly to the improved fracture toughness in the sense that the interface between the components' splats was enhanced, which has been clarified through morphology study shown in Fig. 8. Significantly improved fracture property exhibited by the spheroidized coating shown in Fig. 11 further allude to the importance of splats' interface in influencing coating mechanical property. Therefore, it is believed that the main reinforcement mechanism of the present bioceramic composite coatings is crack deflection or impediment. From this viewpoint, limited chemical reaction is beneficial together with the consideration that it is possible that during medical service of the composite coatings, releases of titania or YSZ particles would be avoided. Also, the reaction layer could act as an underlying support structure during its application, and hence, improve the overall strength of the implant.

From the present study, it was revealed that the processing conditions were responsible for the microstructure of resultant coatings, and hence influenced the mechanical and biological properties. As an alternative to improve the properties of the as sprayed HA coatings, the composite coating is an attractive way towards achieving improved mechanical properties of the calcium phosphate coatings through incorporation of bioinert ceramic additives. However, it should be noted that the additives must be suitably selected in terms of type, incorporation mode, and content. Extent of the chemical reaction between HA and additives would be an important factor determining the ultimate structure, and hence, strength of the resultant composite coatings. As a summary, an overview graph is drawn to portray the significant dependence of both mechanical properties and phase composition of the HVOF HA and HA/titania (YSZ) coatings on processing condition. The graph is shown in Fig. 12, in which the comparison with plasma sprayed HA coatings is also illustrated. Generally, other reports also pointed out that, with content increase of the bioinert additives, mechanical properties of the corresponding composite coatings are effectively augmented [37,38]. The present study further revealed the importance of reactivity of the additives with HA. Additionally, combined with the aforementioned points on strengthening mechanisms of the bioinert ceramic, small particle size could be beneficial for the improvement of mechanical properties. On the other hand, the relationship can also be used to effectively predict coating property and optimize thermal spray processing.

4. Conclusions

The relation among processing parameters, microstructure, and property of HVOF sprayed HA, HA/titania, and HA/YSZ composite coatings was discussed in fair detail in this paper. The results showed that, for pure HA coatings, processing conditions, including starting powder size, exhibited significant effect on the structure of resultant coatings, and hence their mechanical properties. The influence of processing on microstructure was achieved mainly through different melt state of the powders during coating deposition. It is therefore possible that a future refine study can found a relatively accurate relation between extent of HA transformation and melt state of separate HA particles. The incorporation of ceramic additives, YSZ and titania, showed promising effect on improving mechanical performances of HA-based coatings. However, it was revealed that chemical reactions between zirconia and HA or titania and HA cannot be avoided during the coating formation. Even though it was generally

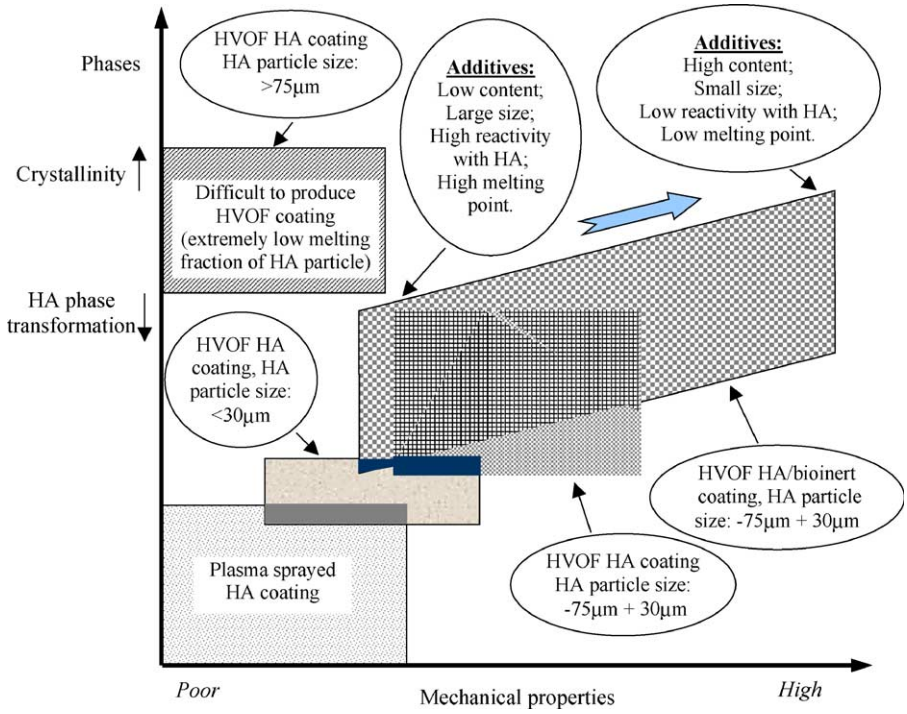

Fig. 12. An overview of dependence of both mechanical properties and phase composition of the HVOF sprayed bioceramic coatings on processing conditions.

believed that the chemical resultants have detrimental effect on biological performances of the composites, the chemical reaction layer, which was clarified in the present study, nevertheless has beneficial contribution to improved structure and mechanical properties. A general overview was proposed to explicate the relations among the processing parameters, microstructure, and properties of the HVOF sprayed bioceramic coatings.

Acknowledgements

The authors thank Mr. K.W. Ling for his help in coating sample preparation. The financial support from Nanyang Technological University of Singapore is acknowledged.

References

[1] Hench LL, Ethridge EC. Biomaterials, an interfacial approach. Academic Press: USA, 1982.
[2] Yagi K, Tokuda M, Suzuki K, Yoshidome H. Evaluation of strength property of HAp-Tyranno fiber composite by flexural test and process of sintering condition. Micromechatronics and Human Science, Proceedings of 1999 International Symposium on MHS'99, 1999. pp. 07–12.
[3] Hardy DCR, Frayssinet P, Delince PE. Osteointegration of hydroxyapatite-coated stems of femoral prostheses. Eur J Orthop Surg Traumatol 1999;9:75–81.
[4] Yoshikawa T, Ohgushi H, Tamai S. Immediate bone forming capability of prefabricated osteogenic hydroxyapatite. J Biomed Mater Res 1996;32:481–92.
[5] Suominen E, Aho AJ, Vedel E, Kangasniemi I, Uusipaikka E, Yli-Urpo A. Subchondral bone and cartilage repair with bioactive glasses, hydroxyapatite, and hydroxyapatite-glass composite. J Biomed Mater Res 1996;32:543–51.
[6] Ducheyne P, Radin S, King L. The effect of calcium phosphate ceramic composition and structure on in vitro behavior, I. Dissolution. J Biomed Mater Res 1993;27:25–34.
[7] Maxian SH, Zawadsky JP, Dunn MG. In vitro evaluation of amorphous calcium phosphate and poorly crystallized hydroxyapatite coatings on titanium implants. J Biomed Mater Res 1993;27:111–7.
[8] Cleries L, Fernandez-Pradas JM, Morenza JL. Behavior in simulated body fluid of calcium phosphate coatings obtained by laser ablation. Biomaterials 2000;21:1861–5.
[9] Brown SR, Turner IG. Acoustic emission analysis of thermal sprayed hydroxyapatite coatings examined under four point bend loading. Surf Eng 1998;14:309–13.
[10] Steinhauser S, Wielage B. Composite coatings: manufacture, properties and application. Proceedings of the 10th Conference on Surface Modif Technology, 1997, Singapore, p. 436–50.
[11] Suchanek W, Yashima M, Kakihana M, Yoshimura M. Hydroxyapatite ceramics with selected sintering additives. Biomaterials 1997;18:923–33.
[12] Silva VV, Lameiras FS, Domingues RZ. Microstructural and mechanical study of zirconia-hydroxyapatite (ZH) composite ceramics for biomedical applications. Composites Sci Technol 2001;61:301–10.
[13] Chou BY, Chang E. Plasma-sprayed hydroxyapatite coating on titanium alloy with ZrO_2 second phase and ZrO_2 intermediate layer. Surf Coat Technol 2002;153:84–92.
[14] Aoki H. Medical Applications of Hydroxyapatite. Ishiyaku EuroAmerica, Inc., Tokyo, St. Louis, 1994.

[15] Chang E, Chang WJ, Wang BC, Yang CY. Plasma spraying of zirconia-reinforced hydroxyapatite composite coatings on titanium: part II dissolution behavior in simulated body fluid and bonding degradation. J Mater Sci Mater Med 1997; 8:201–11.
[16] Weng J, Liu X, Zhang X, Ji X. Thermal decomposition of hydroxyapatite structure induced by titanium and its dioxide. J Mater Sci Lett 1994;13:159–61.
[17] Anh Vu T, Heimann RB. Influence of the CaO/TiO_2 ratio on thermal stability of hydroxyapatite in the system $Ca_5(PO_4)_3OH$–CaO–TiO_2. J Mater Sci Lett 1997;16:1680–2.
[18] Ranganath S. A review on particulate-reinforced titanium matrix composites. J Mater Sci 1997;32:1–16.
[19] Berndt CC, Yi JH. Strength enhancement of plasma sprayed coatings. In: Houck DL, editor. Proceedings of NTSC, USA, 1987. p. 297–308.
[20] Mencik J. Mechanics of components with treated or coated surfaces. Dordrecht: Kluwer Academic Publishers, 1996.
[21] Li H, Khor KA, Cheang P. Young's modulus and fracture toughness determination of HVOF sprayed bioceramic coatings. Surf Coat Technol 2002;155:21–32.
[22] Wang Y. Preparation of functionally graded bioceramic coatings. Master thesis. Nanyang Technological University, Singapore, 1997.
[23] Ogiso M, Yamashita Y, Matsumoto T. Differences in microstructural characteristics of dense HA and HA coating. J Biomed Mater Res 1998;41:296–303.
[24] McPherson R, Gane N, Bastow TJ. Structural characterization of plasma-sprayed hydroxylapatite coatings. J Mater Sci Mater Med 1995;6:327–34.
[25] Lopes MA, Santos JD, Monteriro FJ, Knowles JC. Glass-reinforced hydroxyapatite: a comprehensive study of the effect of glass composition on the crystallography of the composite. J Biomed Mater Res 1998;39:244–51.
[26] Lausma J, Mattsson L, Rolander U. Chemical composition and morphology of titanium surface oxides. In: Williams JM, editor. Biomedical Materials, vol. 55, 1986. p. 351–9.
[27] Campbell AA, Fryxell GE, Linehau JC, Graff GL. Surface-induced mineralization: a new method for producing calcium phosphate coatings. J Biomed Mater Res 1996;32:111–8.
[28] Ramachandra Rao R, Kannan TS. Synthesis and sintering of hydroxyapatite-zirconia composites. Mater Sci Eng C 2002;20:187–93.
[29] Chou BY, Chang E, Yao SY, Chen JM. Phase transformation during plasma spraying of hydroxyapatite-10-wt%-zirconia composite coating. J Am Ceram Soc 2002;85:661–9.
[30] Khor KA, Fu L, Lim VJP, Cheang P. The effects of ZrO_2 on the phase compositions of plasma sprayed HA/YSZ composite coatings. Mater Sci Eng A 2000;276:160–6.
[31] Grassmann O, Heimann RB. Compositional and microstructural changes of engineered plasma-sprayed hydroxyapatite coatings on Ti6Al4V substrates during incubation in protein-free simulated body fluid. J Biomed Mater Res 2000;53:685–93.
[32] Lopes MA, Santos JD, Ohtsuki FJ, Osaka A, Kaneko S, Inoue H. Push-out testing and histological evaluation of glass reinforced hydroxyapatite composites implanted in the tibia of rabbits. J Biomed Mater Res 2001;54:463–9.
[33] Turi EA. Thermal characterization of polymeric materials, 2nd edition. San Diego: Academic Press, 1997.
[34] Callus PJ, Berndt CC. Relationships between the mode II fracture toughness and microstructure of thermal spray coatings. Surf Coat Technol 1999;114:114–28.
[35] Li CJ, Ohmori A, McPherson R. Relationship between microstructure and Young's modulus of thermally sprayed ceramic coatings. J Mater Sci 1997;32:997–1004.
[36] Metsger DS, Rieger MR, Foreman DW. Mechanical properties of sintered hydroxyapatite and tricalcium phosphate ceramic. J Mater Sci Mater Med 1999;10:9–17.
[37] Kong YM, Kim S, Kim HE, Lee IS. Reinforcement of hydroxyapatite bioceramic by addition of ZrO_2 coated with Al_2O_3. J Am Ceram Soc 1999;82:2963–8.
[38] Lim VJP, Khor KA, Fu L, Cheang P. Hydroxyapatite-zirconia composite coatings via the plasma spraying process. J Mater Process Technol 1999;89-90:491–6.